



---

Interhemispheric Correlation of Late Pleistocene Glacial Events

Author(s): T. V. Lowell, C. J. Heusser, B. G. Andersen, P. I. Moreno, A. Hauser, L. E. Heusser, C. Schlüchter, D. R. Marchant, G. H. Denton

Source: *Science*, New Series, Vol. 269, No. 5230 (Sep. 15, 1995), pp. 1541-1549

Published by: American Association for the Advancement of Science

Stable URL: <http://www.jstor.org/stable/2889102>

Accessed: 15/07/2009 15:01

---

Your use of the JSTOR archive indicates your acceptance of JSTOR's Terms and Conditions of Use, available at <http://www.jstor.org/page/info/about/policies/terms.jsp>. JSTOR's Terms and Conditions of Use provides, in part, that unless you have obtained prior permission, you may not download an entire issue of a journal or multiple copies of articles, and you may use content in the JSTOR archive only for your personal, non-commercial use.

Please contact the publisher regarding any further use of this work. Publisher contact information may be obtained at <http://www.jstor.org/action/showPublisher?publisherCode=aaas>.

Each copy of any part of a JSTOR transmission must contain the same copyright notice that appears on the screen or printed page of such transmission.

JSTOR is a not-for-profit organization founded in 1995 to build trusted digital archives for scholarship. We work with the scholarly community to preserve their work and the materials they rely upon, and to build a common research platform that promotes the discovery and use of these resources. For more information about JSTOR, please contact [support@jstor.org](mailto:support@jstor.org).



*American Association for the Advancement of Science* is collaborating with JSTOR to digitize, preserve and extend access to *Science*.

<http://www.jstor.org>

# Interhemispheric Correlation of Late Pleistocene Glacial Events

T. V. Lowell, C. J. Heusser, B. G. Andersen, P. I. Moreno,  
A. Hauser, L. E. Heusser, C. Schlüchter,  
D. R. Marchant, G. H. Denton

A radiocarbon chronology shows that piedmont glacier lobes in the Chilean Andes achieved maxima during the last glaciation at 13,900 to 14,890, 21,000, 23,060, 26,940, 29,600, and  $\geq 33,500$  carbon-14 years before present ( $^{14}\text{C}$  yr B.P.) in a cold and wet Subantarctic Parkland environment. The last glaciation ended with massive collapse of ice lobes close to 14,000  $^{14}\text{C}$  yr B.P., accompanied by an influx of North Patagonian Rain Forest species. In the Southern Alps of New Zealand, additional glacial maxima are registered at 17,720  $^{14}\text{C}$  yr B.P., and at the beginning of the Younger Dryas at 11,050  $^{14}\text{C}$  yr B.P. These glacial maxima in mid-latitude mountains rimming the South Pacific were coeval with ice-rafting pulses in the North Atlantic Ocean. Furthermore, the last termination began suddenly and simultaneously in both polar hemispheres before the resumption of the modern mode of deep-water production in the Nordic Seas. Such interhemispheric coupling implies a global atmospheric signal rather than regional climatic changes caused by North Atlantic thermohaline switches or Laurentide ice surges.

Detailed oxygen-isotope records from Greenland ice cores show repeated millennial-scale temperature oscillations, called Dansgaard-Oeschger events, between glacial stadials and interstadials (1–3). Each stadial begins either gradually or with stepwise changes and then ends abruptly. Sea-surface temperatures estimated from microfossils in North Atlantic sediment cores exhibit oscillations that match those in the ice cores (4). In both the ice and sediment cores, oscillations older than 20,000  $^{14}\text{C}$  yr B.P. are grouped into longer cooling hemicycles, each followed by pronounced warming. In addition, some North Atlantic sediment cores show evidence of Heinrich events in the form of sea-surface cooling, lowered surface salinities, increased ice-rafted detritus, and reduced foraminiferal fluxes (5, 6). Because of their association with prominent layers of ice-rafted detrital carbonate, Heinrich events are commonly attributed to massive discharges of Laurentide icebergs through the Hudson Strait (6). Heinrich events H-2 through H-6 each oc-

curred near the culmination of a long cooling trend (4). Heinrich event H-1, which occurred at 13,700 to 14,900  $^{14}\text{C}$  yr B.P., marked the end of a prolonged interval of glacial climate (4). The expression of the Younger Dryas event in some North Atlantic sediment cores resembles that of the Heinrich events (4).

Because the abrupt changes recorded in Greenland ice and North Atlantic sediments so far appear to have been areally restricted, most explanations have invoked regional mechanisms. For example, Dansgaard-Oeschger events have been attributed to variations of North Atlantic thermohaline downwelling tied to the discharge of meltwater and icebergs (7), and Heinrich events to subglacial freezing and thawing of soft basal sediments in Hudson Bay and Hudson Strait that produced Laurentide ice-stream surges (8). It has also been proposed that variations in thermohaline circulation caused by unstable discharge of all portions of the Laurentide Ice Sheet that rested on deforming sediments is the ultimate cause of abrupt North Atlantic climate changes (9).

Quite a different perspective on these abrupt climate shifts would emerge if it turns out that they were registered globally. Tight interhemispheric coupling of temperature changes would implicate global rather than regional forcing mechanisms. In this research article, we report radiocarbon dates of Andean glacier and vegetation fluctuations in the Chilean Lake District and on Isla Grande de Chiloé, complemented by data from the Southern Alps of New Zealand. Both regions are adjacent to the Pacific Ocean; both are at  $41^\circ$  to  $44^\circ\text{S}$  latitude

and thus within the influence of the Southern Hemisphere westerlies; both are far from the North Atlantic region, large ice sheets, and sources of thermohaline downwelling; and both feature mid-latitude mountain glaciers that receive high precipitation and respond quickly to climatic change. Thus the Chilean Andes and the Southern Alps are prime localities for determining whether the North Atlantic climatic pulses were regional events or were part of a global signature.

**Llanquihue glacier advances in the Chilean Andes.** The wide, flat-floored longitudinal valley that trends north-south along the western flank of the Chilean Andes shows several major topographic features related to the last (Llanquihue) glaciation in the Lake District and on Isla Grande de Chiloé (Fig. 1). Here a complex belt of Llanquihue-age moraines delineates former piedmont glaciers that flowed westward from the Andes into the longitudinal valley. Graded to the distal portion of the Llanquihue moraine belt are extensive outwash plains. Together, the Llanquihue moraines and outwash represent glacial maxima when the Andean snowline was depressed about 1000 m below present values (10). Nested behind the Llanquihue moraine belt are the deep Rupanco, Llanquihue, Seno Reloncaví, Ancud, and Castro basins. Piedmont ice lobes with gentle surface slopes filled these basins at Llanquihue glacial maxima. Lakes or marine gulfs flooded the basins when the ice lobes collapsed during the last termination.

The Llanquihue moraine belt features discontinuous cross-cutting ridges, along with palimpsest landforms. The moraine ridges stand 3.0 to 20 m high, and many have well-preserved ice-contact slopes. Most moraine cores are composed of gravelly sediment flows derived from an adjacent ice snout. Some cores were folded and faulted by advancing Llanquihue ice. Till layers from 0.80 to 3.0 m thick are commonly distributed across the proximal moraine slopes and in many cases cover the moraine crests. These tills are light gray, compact, and contain numerous striated clasts of andesite and granite derived from the Andes. They are discontinuous and little weathered; many exhibit shear planes and boudinage structures. Most are basal lodgement tills, although some are meltout or flow tills. At the eastern margin of the moraine belt, an ice-contact slope rises as much as 60 to 130 m above the glacial lakes and marine embayments. Banked against this ice-contact slope are complex sets of kame terraces; some have been partly sheared off and capped with till, whereas others are intact.

Individual drift sheets within the Llanquihue moraine belt can be traced for only

T. V. Lowell is in the Department of Geology, University of Cincinnati, Cincinnati, Ohio 45221, USA. C. J. Heusser is at Clinton Woods, Tuxedo, NY 10987, USA. B. G. Andersen is in the Institute for Geology, University of Oslo, Post Office Box 1047, Blindern N-0316, Oslo, Norway. P. I. Moreno is in the Department of Plant Biology and Pathology and Institute for Quaternary Studies, University of Maine, Orono, ME 04469, USA. A. Hauser is with the Servicio Nacional de Geología y Minería, Casilla 10465, Santiago, Chile. L. E. Heusser is with Lamont-Doherty Earth Observatory of Columbia University, Palisades, NY 10964, USA. C. Schlüchter is in the Institute for Geology, University of Bern, Bern, Switzerland. D. R. Marchant is in the Institute for Quaternary Studies, University of Maine, Orono, ME 04469, USA. G. H. Denton is in the Department of Geological Sciences and Institute for Quaternary Studies, University of Maine, Orono, ME 04469, USA.

a few hundred meters. Some moraine ridges were overrun by Llanquihue ice, and others are composite features from several Llanquihue advances. Some ice-contact slopes have been occupied more than once; others have been overrun. In places beyond the former ice terminus, Llanquihue outwash has been folded into linear ridges that resemble ice-marginal features. Therefore, rather than attempting to delineate the areal extent of individual drift sheets, we produced detailed morphologic maps of Llanquihue moraine belts and outwash plains. These maps served as the basis for plotting stratigraphic sections, radiocarbon samples, and pollen stratigraphies from sediment cores located within the moraine belt, hence guiding reconstruction of Llanquihue ice-margin fluctuations (Fig. 1, Table 1). The mapping and radiocarbon dates show that the Llanquihue moraines and outwash plains belong to the last global glaciation and that at least six Llanquihue glacier advances reached the outer moraine belt.

The youngest well-dated Llanquihue glacier advance into the outer moraine belt culminated at 13,900 to 14,890  $^{14}\text{C}$  yr B.P. and is best documented for the Lago Llanquihue and Castro piedmont lobes. In this advance the Lago Llanquihue piedmont glacier reached its maximum at the outer edge of a kame terrace banked against the lakeside ice-contact slope; this terrace consists of outwash and lacustrine sediment discharged from the adjacent piedmont ice lobe. According to Porter (10), lahars that cover the southern part of the terrace were derived from the volcano Calbuco; they flowed around the ice margin on the top of the terrace and exited the Llanquihue basin through the river outlet while the piedmont ice lobe still stood at the outer edge of the terrace. At Llanquihue (site 1 in Fig. 1 and Table 1) the error-weighted mean age of eight wood samples buried by ice-proximal glaciofluvial deposits shows that construction of the ice-marginal terrace began at 14,890  $^{14}\text{C}$  yr B.P. (11). At Puerto Varas (site 2), radiocarbon dates of about 14,500  $^{14}\text{C}$  yr B.P. from wood and organic silt register a break in terrace construction and therefore could suggest brief ice withdrawal from the terrace margin. Also at Puerto Varas the error weighted mean age of five wood and fibrous peat samples (Table 1) from just beneath the capping lahars indicates that the terrace was still under construction as late as 14,240  $^{14}\text{C}$  yr B.P. (11, 12).

At Dalcahue on Isla Grande de Chiloé (site 3), we dated wood and organic silt samples from 1.52 m of organic silt that accumulated in a wet depression now beneath a Llanquihue moraine ridge. Organic accumulation was terminated by an advance of the Castro piedmont glacier lobe that left an initial layer of fine-to-medium

sand, followed by coarser glaciofluvial deposits that form the core of the overlying Llanquihue moraine. Till with striated granite boulders derived from the Andes caps the moraine. The surface of the Dalcahue organic silt bed is preserved intact under the initial sand layer. Thirty-five radiocarbon samples of wood and fibrous organic material from this former land surface yield an error-weighted mean age of 14,810

$^{14}\text{C}$  yr B.P. (11), which dates a Llanquihue glacier advance of the Castro piedmont lobe onto Isla Grande de Chiloé (11) [see (13, 14) for earlier radiocarbon dates of the Dalcahue organic bed]. This advance culminated near the lip of a prominent ice-contact slope (site 4) located 2.0 km west of the Dalcahue site. Radiocarbon dates show that the accumulation of the Dalcahue organic silt extended back continuously from

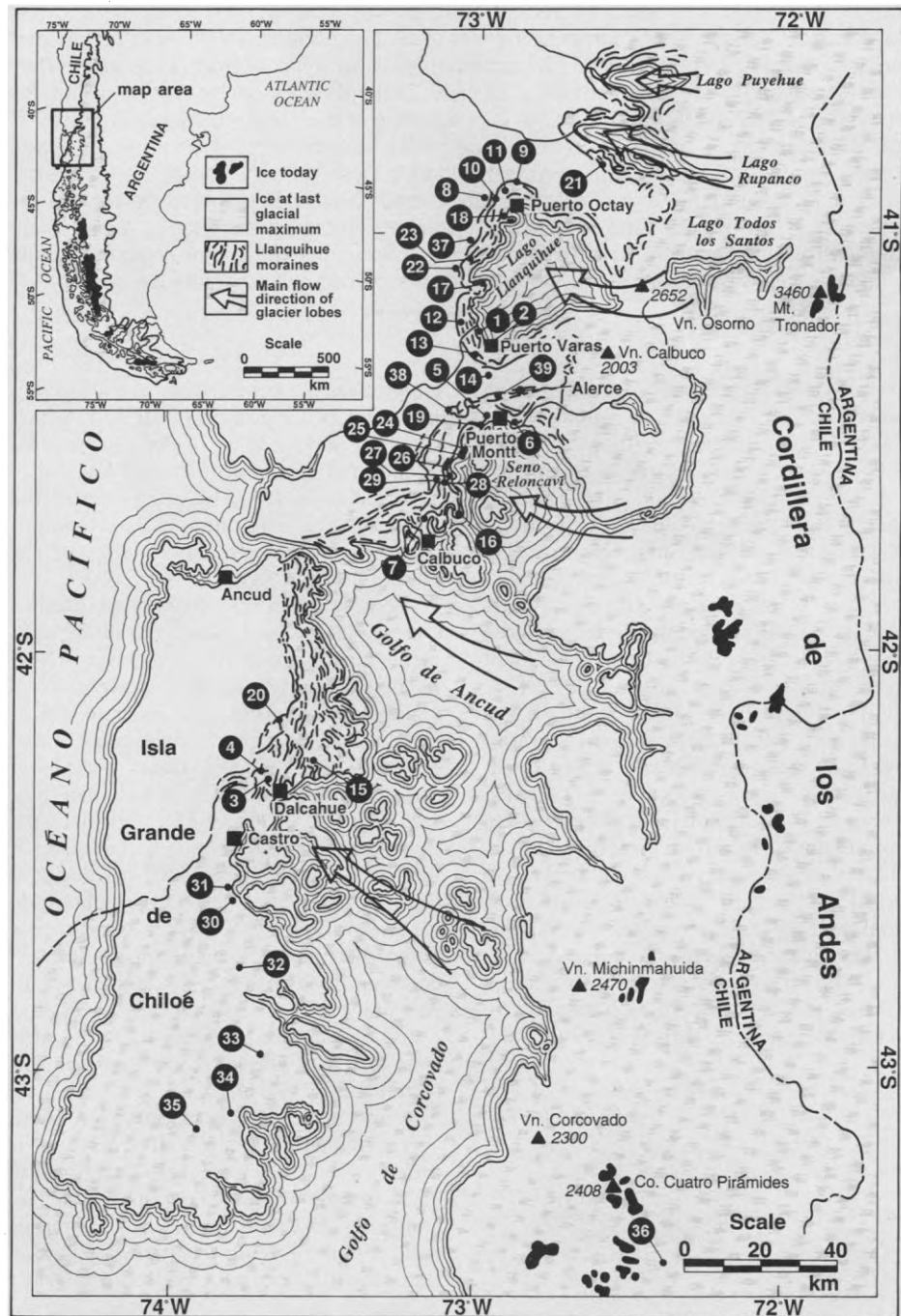


**Fig. 1.** Schematic map of the Llanquihue moraine system in the Chilean Lake District and on Isla Grande de Chiloé. The site numbers refer to the text and to Table 1. The ice extent for the last glacial maximum shown in the inset is from (49). This schematic map is based on detailed glacial geologic maps constructed at a scale of 1:64,500 of the entire Llanquihue-age moraine belt from Lago Puyehue in the north to Castro on Isla Grande de Chiloé in the south.

14,810 to at least 30,070  $^{14}\text{C}$  yr B.P. (Table 1). Hence the overriding at 14,810  $^{14}\text{C}$  yr B.P. represents the most extensive advance achieved by the Castro lobe through this entire interval. The age of the 14,810- $^{14}\text{C}$ -yr-B.P. advance at Dalcahue is in accord with the initial construction of the lakeside kame terrace at Llanquihue at 14,890  $^{14}\text{C}$  yr B.P. (11).

The intervening Seno Reloncaví and Ancud piedmont glacier lobes both advanced toward a maximum after about 15,000  $^{14}\text{C}$  yr B.P. At Puerto Montt this advance reached the top of the ice-contact slope that rises above the gulf, as indicated by radiocarbon ages as young as 15,040  $^{14}\text{C}$  yr B.P. for reworked organic clasts in an outwash plain that heads at the ice-contact slope (site 5). Consistent with this interpretation is till at Punta Penas near Puerto Montt, which is smeared across lacustrine sediments with an enclosed organic silt layer dated to 16,000  $^{14}\text{C}$  yr B.P. (site 6). Near Calbuco (site 7), reworked organic clasts in deltaic deposits beneath till show that the Ancud lobe advanced into the Llanquihue moraine belt after 15,285 to 15,500  $^{14}\text{C}$  yr B.P. Taken together, the radiocarbon dates from near Puerto Montt and Calbuco suggest that the Seno Reloncaví and Ancud piedmont glaciers expanded coincident with advance of the Lago Llanquihue and Castro piedmont lobes. Overall this advance was relatively more extensive for the southern than for the northern piedmont lobes.

The next-older dated Llanquihue advance culminated close to 21,000  $^{14}\text{C}$  yr B.P. It is best documented for the Lago Llanquihue, Castro, and Seno Reloncaví piedmont glacier lobes. We dated organic clasts reworked into outwash graded to the outermost Llanquihue moraine and ice-contact slope of the northwestern portion of the former Lago Llanquihue piedmont glacier (sites 8 and 9). The resulting maximum ages for this ice-marginal position are 20,840 and 23,020  $^{14}\text{C}$  yr B.P. We obtained minimum ages for ice recession of 20,160 to 20,580  $^{14}\text{C}$  yr B.P. from basal organic matter in two abandoned meltwater spillway channels that originated at the lakeside ice-contact slope and cut through the outer Llanquihue moraines (sites 10 and 11).

Drift deposited by the southwestern part of the former Lago Llanquihue piedmont lobe yields a similar chronology. Here basal organic material from the Fundo Llanquihue sediment core on the proximal side of the outermost Llanquihue moraine gave radiocarbon dates of 20,455 to 20,890  $^{14}\text{C}$  yr B.P. (site 12). Reworked organic material from beneath a continuation of this moraine 6 km south of Fundo Llanquihue afforded ages as young as 25,020  $^{14}\text{C}$  yr B.P. (site 13). An outwash plain graded to this same moraine yielded reworked organic

clasts with ages of 22,250 and 22,985  $^{14}\text{C}$  yr B.P. (site 14), giving a close maximum age for the ice limit. Overall, these radiocarbon dates document a Llanquihue maximum at close to 21,000  $^{14}\text{C}$  yr B.P. The ice-margin position at 21,000  $^{14}\text{C}$  yr B.P. was here about 4 km beyond the margin of the Lago Llanquihue piedmont lobe when it terminated at the lakeside kame terrace.

At Teguaco on Isla Grande de Chilóe (site 15), a roadcut in a southeastward-draining river valley reveals organic silt overlain sharply by gray, laminated glaciolacustrine silt, which in turn grades upward into ice-proximal glaciofluvial sediments. The sequence represents an incursion of the Castro piedmont glacier onto eastern Isla Grande de Chilóe, first damming lakes in river valleys and then advancing over the Teguaco site and into the outer Llanquihue moraine belt. Twelve radiocarbon samples for a drowned organic trash layer on the upper surface of the organic silt, and for wood fragments in the glaciolacustrine silt, yield an error-weighted mean age of 22,300  $^{14}\text{C}$  yr B.P. (11). We interpret these radiocarbon dates to mean that at about 22,300  $^{14}\text{C}$  yr B.P. the Castro lobe advanced onto eastern Isla Grande de Chilóe toward a Llanquihue glacial maximum. The radiocarbon dates from the Dalcahue organic silt bed show that this advance terminated behind the position subsequently reached at 14,810  $^{14}\text{C}$  yr B.P. Finally, a radiocarbon age of shells from glaciomarine sediments that were thrust into a moraine core demonstrates that the intervening Seno Reloncaví piedmont glacier lobe advanced into the outer Llanquihue moraine belt at 20,925  $^{14}\text{C}$  yr B.P. (site 16).

A Llanquihue advance that culminated at about 26,940  $^{14}\text{C}$  yr B.P. is documented near Frutillar Bajo alongside Lago Llanquihue (site 17). Here a section near the top of the lakeside ice-contact slope reveals two till units separated by 95 cm of organic silt, which accumulated in a wet depression on the surface of the lower till. Organic accumulation was terminated by advancing Llanquihue glacier ice that sheared off the lakeside end of the organic bed and deposited till over the surviving organic silt. This compact till reaches 3 m in thickness and has numerous internal shear planes and boudinage structures. For about 6 m of lateral exposure, the base of the till is separated from the surface of the underlying organic silt not by a shear plane but by a silty sediment flow and a thin gravel lens derived from the advancing glacier margin. These deposits buried intact the grass-covered land surface of the surviving portion of the organic silt bed. Thirteen radiocarbon dates of fossil grass and litter from this surface give an error-weighted mean age of 26,940  $^{14}\text{C}$  yr B.P. for an advance of the Lago

Llanquihue piedmont glacier to within 2 km of the outer edge of the Llanquihue moraine belt (11). In addition, the lower Llanquihue till at the Frutillar Bajo site represents an earlier glacier advance to within 2 km of the outer limit of the moraine belt prior to 34,765 to 36,960  $^{14}\text{C}$  yr B.P., the ages for the basal organic silt.

A roadcut near Puerto Octay reveals two superimposed ice-proximal outwash units deposited when a former piedmont glacier lobe stood at the top of the ice-contact slope above Lago Llanquihue within 2.2 km of the outer limit of the Llanquihue moraine belt (site 18). The two outwash units are separated by a 90-cm-thick organic silt unit with an exposed lateral extent of 125 m. The upper surface of the organic silt at differing sites along the exposure yielded five radiocarbon dates with an error-weighted mean of 29,360  $^{14}\text{C}$  yr B.P. (11) (Table 1). This upper surface does not exhibit a fossil grass and litter layer. However, the consistency of the radiocarbon ages implies that little material has been eroded off the organic bed. Ages increase markedly with depth within the organic silt, and hence the upper surface would have yielded highly disparate ages if even only a few centimeters of silt had been removed. Therefore the age of about 29,360  $^{14}\text{C}$  yr B.P. probably affords a close limiting date for deposition of the upper outwash, which represents glacier advance to the top of the ice-contact slope. Four radiocarbon dates of the basal organic silt at differing sites along the exposure yield limiting minimum ages for the lower outwash unit (and therefore for an advance to the top of the ice-contact slope) of 33,900 to 39,340  $^{14}\text{C}$  yr B.P. Overall, this exposure near Puerto Octay reveals an interstadial organic silt bed dated at  $\geq 39,340$  to 29,360  $^{14}\text{C}$  yr B.P. between two ice-proximal outwash units, each representing an extensive piedmont glacier lobe.

A sequence of glaciofluvial units is stacked on an ice-contact slope that rises 130 m above Seno Reloncaví at Puerto Montt (site 19). The seaward portion of the stacked sequence has been truncated by shearing during a glacier advance to the outer Llanquihue moraine belt. The glaciofluvial units are each separated by a peat or gyttja bed with upper and lower surfaces that have not been eroded. We infer that the ice-proximal glaciofluvial units over each of the upper two organic beds represent advances of the Seno Reloncaví piedmont glacier onto the ice-contact slope. In this context, two dates of the upper surface of the highest peat bed afford a mean age of 23,060  $^{14}\text{C}$  yr B.P.; six samples from the upper surface of the next-highest peat bed yielded an error-weighted mean age of 29,600  $^{14}\text{C}$  yr B.P. for another advance (11).

At four localities glacial deposits date

from ice advances into the outer Llanquihue moraine belt at  $\geq 33,500$   $^{14}\text{C}$  yr B.P. We assign a Llanquihue age to these deposits because they are little weathered and because pollen profiles from overlying organic-rich sediments show no evidence for full interglacial conditions. We discussed the sites at Frutillar Bajo and Puerto Octay above. A third locality is at site 13 (Fig. 1). Here thick Llanquihue outwash older than  $33,400$   $^{14}\text{C}$  yr B.P. represents an advance to

within 1 km of the  $21,000$ - $^{14}\text{C}$ -yr-B.P. ice-marginal position and 4 km beyond the  $14,890$ - $^{14}\text{C}$ -yr-B.P. position. Finally, basal organic material from a mire at Taiquemó on Isla Grande de Chiloé (site 20) shows that here the outermost Llanquihue moraine is  $>49,892$   $^{14}\text{C}$  yr B.P. in age. This ice-marginal position is just distal to that reached by the  $14,810$ - $^{14}\text{C}$ -yr-B.P. advance.

Overall, we recognize at least six glacier advances into the outer Llanquihue mo-

raine belt at  $14,890$ ,  $21,000$ ,  $23,060$ ,  $26,940$ ,  $29,600$ , and  $\geq 33,500$   $^{14}\text{C}$  yr B.P. Two of these advances are documented for three piedmont glacier lobes, and the remainder for one or two lobes (Fig. 2). In an earlier study, Mercer (15) pointed out that the outer Llanquihue moraine of the former Lago Rupanco piedmont glacier lobe rested on ash-rich peat dated to  $19,450 \pm 300$   $^{14}\text{C}$  yr B.P. The implication is that this glacier lobe reached a maximum at that time.

**Table 1.** Radiocarbon dates associated with glacial deposits in the Chilean Lake District and on Isla Grande de Chiloé from the University of Arizona Laboratory of Isotope Geochemistry (A), the NSF-Arizona Accelerator Mass Spectrometry (AMS) Facility (AA), the University of Georgia Radiocarbon Laboratory (UGA), the Trondheim Laboratoriet for Radiologisk Datering (TUA and T), the University of Washington Quaternary Isotope Laboratory (QL), the University of Waikato Radiocarbon Laboratory (Wk), ETH-Hönggerberg AMS Facility (ETH), and Beta Analytic (Beta). S, site number; Lab No., laboratory

S	Description	Lab No.	Age ( $^{14}\text{C}$ yr B.P.)	$\delta^{13}\text{C}$	S	Description	Lab No.	Age ( $^{14}\text{C}$ yr B.P.)	$\delta^{13}\text{C}$				
1	Llanquihue. Wood from top of interstadial bed beneath lakeside ice-contact terrace. Dates Llanquihue maximum.	ETH-13529	14,850±100*	-25.5	4	Reworked organic silt clast in ice-contact stratified drift at lip of ice-contact head 2 km west of the Dalcahue. Maximum for Llanquihue advance to this site.	QL-4532	14,820±450	-24.5				
		ETH-13530	14,670±120*	-26.6			5	Puerto Montt. Reworked organic silt and small clasts in outwash that heads at ice-contact slope alongside Seno Reloncavi. Maximum for Llanquihue advance.	A-6491	16,900±120	-25.9		
		ETH-13531	14,810±120*	-22.9					A-6492	15,640±100	-27.5		
		ETH-13532	14,780±120*	-21.7					A-6493	15,040±100	-25.2		
		ETH-13533	14,930±120*	-24.1					UGA-6942	16,060±120	-25*		
		ETH-13534	15,120±140*	-20.9					6	Punta Penas. Organic silt layer within lacustrine sediments overlain by till. Maximum for Llanquihue advance.	T-10296A	15,940±315	-27.6
A-8173	15,120±95	-28.0	T-10297A	16,275±440	-28.9								
A-8174	14,750±80	-27.9	T-10298A	16,000±275	-27.5								
2	Puerto Varas. Wood and organic silt from within lakeside ice-contact terrace. Dates short cessation of glacial lacustrine sedimentation in terrace at Bella Vista Bluff.	A-6322	14,430±140	-24.8	7	Reworked peat clasts in foreset bed of proglacial delta that is covered with till. Maximum for Llanquihue advance.	A-7702	15,285±150/-145	-25.8				
		T-9656A	14,560±95	-27.6			A-7698	15,500±85	-26.1				
3	Puerto Varas. Wood and fibrous peat from near top of lakeside ice-contact terrace at railroad bridge location. Affords age when piedmont ice still stood at edge of terrace	ETH-13528	14,290±100*	-24.8	8	Reworked peat clasts in outwash that grades to moraine ridge on top of prominent ice-contact slope. Maximum for outermost Llanquihue moraine.	QL-4527	20,840±400	-25.5				
		AA-7459 B	13,940±85*	-25*			Wk-2539	27,700±200	-27.0				
		AA-7460	14,175±110*	-25*	9	Peat clast reworked into outwash beneath till. Maximum for outermost Llanquihue moraine.	QL-4539	23,020±280	-24.8				
		AA-7465	14,600±110*	-25*			10	Macrofossils from base of 4.8-m core in a mire within a meltwater spillway. Minimum for outermost Llanquihue moraine.	AA-9296	20,160±180*	-27.2		
		AA-7465C	14,350±90*	-25*					11	Macrofossils from base of two 2.7-m cores in a mire within a meltwater spillway. Minimum for outermost Llanquihue moraine.	AA-9298	20,380±170*	-29.9
		A-6189	14,720±100	-27.8			AA-9303	20,580±170*			-29.9		
		A-6190	14,770±110	-27.7			12	Fundo Llanquihue. Macrofossils from base of an 11-m core in a mire situated on the proximal side of the outermost Llanquihue moraine. Minimum for outermost Llanquihue moraine.	UGA-6907	20,645±220*	-20.8		
		A-7716	15,045±80	-26.7					UGA-6908	20,890±185*	-21.2		
		A-7727	14,915±75	-27.9					UGA-6909	20,455±180*	-15.4		
		UGA-6822	14,610±180	-29.4					UGA-6910	20,650±175*	-23.1		
		UGA-6823	15,050±180	-27.4					UGA-6912	20,680±175*	-23.5		
		UGA-6824	14,700±170	-27.6					UGA-6913	20,585±170*	-24.9		
		UGA-6825	14,620±180	-27.6					13	Remobilized organic silt beneath moraine. Maximum for outermost Llanquihue moraine.	UGA-6939	25,020±290	-26.5
		UGA-6971	15,155±125	-26.6							UGA-7092	25,680±330	-25*
		UGA-6918	14,480±180	-28.1	UGA-6821	26,150±220	-24.4						
		UGA-6921	14,520±105	-26.0	A-7662	33,400±395/-375	-25.0						
		UGA-6922	14,995±100	-26.8	14	Peat clasts reworked into outwash that grades to outermost Llanquihue moraine. Maximum for moraine.	Wk-2536	22,250±220	-26.9				
		UGA-6933	14,915±105	-26.4			TUA-470A	22,985±235*	-27.7				
		UGA-6983	15,260±115	-27.4	15	Teguaco. Gytja and macro fossils from trash layer on upper surface of organic silt bed that is covered by laminated, light-gray glacial lacustrine, and wood in lacustrine silt. The lacustrine silt is overlain by sand and then ice-proximal glaciofluvial sediments. Dates Llanquihue advance.	AA-13731	22,068±230*	-26.1				
		AA-13710	14,458±98*	-28.6			AA-13732	23,126±207*	-26.4				
AA-13711	14,697±125*	-28.8	AA-13733	22,501±198*			-24.6						
AA-13712	14,799±91*	-28.7	QL-4534	22,400±100			-26.8						
AA-13713	14,689±102*	-28.3	A-7624	22,500±120			-26.3						
AA-13714	14,653±99*	-27.9	A-7623	22,630±125			-26.3						
AA-13715	14,710±130*	-26.9	A-7687	22,075±120			-28.1						
AA-13716	14,862±101*	-27.2	A-7710	21,955±120/-115			-27.9						
AA-13717	14,703±101*	-28.3	A-7729	21,690±120			-28.3						
AA-13718	14,589±101*	-27.3	A-7686	22,410±135/-130			-28.0						
AA-13719	14,663±121*	-28.5	A-7732	22,350±205/-200			-28.4						
AA-13720	14,620±134*	-27.8	A-7719	22,520±170/-165			-27.6						
AA-13721	14,880±99*	-27.1	16	Shells from glaciomarine sediments thrust into the core of a moraine. Dates Llanquihue advance.	A-7627	20,925±115	+1.3						
AA-13722	14,991±100*	-27.6											
	Dalcahue. Organic silt from the base of 152-cm-thick organic bed. Minimum age for penultimate Llanquihue advance over this site.	A-7685	30,070±225/-215	-26.5									

\*Accelerator-mass-spectrometry radiocarbon date. +estimated.

However, the youngest age that we have obtained for organic material from the same borrow pit is  $20,605 \pm 880$   $^{14}\text{C}$  yr B.P. (site 21). Mercer (15) also suggested that the Lago Llanquihue lobe achieved its maximum extent near Frutillar Alto shortly after  $20,100 \pm 500$   $^{14}\text{C}$  yr B.P., the date for a reworked organic clast in outwash that passes beneath till of the outer Llanquihue moraine. However, the youngest organic clast that we have had dated from this outwash

unit from a nearby site is  $21,840 \pm 700$   $^{14}\text{C}$  yr B.P. in age (site 22). In addition, radiocarbon dates at sites 10, 11, and 12 indicate that the former piedmont lobe had retreated from the outer Llanquihue moraine before  $20,160$  to  $20,890$   $^{14}\text{C}$  yr B.P., whereas a date at site 23 indicates recession from the outer moraine before  $19,768$   $^{14}\text{C}$  yr B.P.

**Llanquihue paleoenvironments.** A paleovegetation composite of 10 radiocarbon-dated pollen stratigraphies from the mo-

raine belts of the Lago Llanquihue, Seno Reloncaví, and Castro piedmont glacier lobes shows environmental conditions during the Llanquihue glaciation (Fig. 2). Before the  $14,000$ - $^{14}\text{C}$ -yr-B.P. level, pollen of Subantarctic Parkland plants is predominant in cores or sections from Frutillar Bajo ( $35,000$  to  $26,940$   $^{14}\text{C}$  yr B.P.), the Puerto Octay ice-contact slope ( $36,000$  to  $29,360$   $^{14}\text{C}$  yr B.P.), the Puerto Octay spillway at site 10 (between  $20,180$  and  $14,000$   $^{14}\text{C}$  yr

number;  $\delta^{13}\text{C}$  is in per mil. The dates for samples QL-1338 and QL-1339 are from (10); QL-1012, RL-1892, and GX-3809 are from (50); Beta 10481 and Beta 10485 are from (51). All other radiocarbon dates are new. The conditions for radiocarbon dating are particularly good in this part of Chile because there is no hardwater effect.

S	Description	Lab No.	Age ( $^{14}\text{C}$ yr B.P.)	$\delta^{13}\text{C}$	S	Description	Lab No.	Age ( $^{14}\text{C}$ yr B.P.)	$\delta^{13}\text{C}$											
17	Frutillar Bajo. Organic silt, grass, and surface litter from 7 separate localities along the upper surface of a 95-cm-thick bed of organic silt that separates two till units at the crest of a steep ice-contact slope. Samples from a former land surface preserved intact beneath the upper till. They date a glacial advance into outer Llanquihue moraine belt.	A-7660	26,870±230/-225	-26.8	21	Rupanco. Peat thrust into the core of a moraine ridge. Maximum for outer Llanquihue moraine.	T-9660A	22,560±495	-24.9											
		A-7661	26,560±165	-26.1			T-9659A	20,605±880	-27.7											
		A-7656	27,900±195/-190	-25.6			T-10309A	22,745±295	-26.7											
		UGA-6817	27,425±215*	-26.4			UGA-7092	25,680±330	-25.0											
		UGA-6818	27,305±325*	-25.9			Wk-2537	29,800±300	-27.1											
		UGA-6819	27,855±325*	-25.6			A-6556	28,990±430	-27.4											
		UGA-6820	27,780±335*	-26.8			A-6198	28,450±560	-27.0											
		UGA-6723	26,530±300	-24.8			QL-4549	27,250±250	-26.0											
		AA-13701	26,151±303*	-27.7			QL-4547	24,250±250	-26.1											
		AA-13702	26,809±310*	-27.0			A-6197	22,790±410	-26.6											
18	Puerto Octay. Organic silt from 5 separate localities along the upper surface of a 90-cm-thick layer of organic silt that separates two ice-proximal outwash units near the top of the lakeside ice-contact slope. Both outwash units were derived from an ice lobe that extended to the upper lip of the ice-contact slope. These dates afford age for upper outwash unit and hence glacial maximum.	UGA-6945	34,765±840	-25.0	22	Frutillar Alto. Peat and organic silt clasts reworked into outwash graded to outermost Llanquihue moraine. Maximum ages for outwash and moraine.	AA-13703	26,444±290*	-27.5	QL-4548	21,840±700	-27.1								
		UGA-6919	34,985±440	-25.5			AA-14774	19,768±397*	-18.1	23	Liña Pantanosa. Basal gyttja from core in mire in moraine depression. Minimum age for outermost Llanquihue moraine.	AA-13844	13,295±91*	-28.3						
		UGA-6724	36,960±550	-25.9			24	Basal gyttja from core in moraine depression. Minimum age for recession following the youngest Llanquihue maximum.	AA-13843			13,932±119*	-28.7							
		19	Puerto Octay. Organic silt from four separate localities along the base of the organic silt unit. Minimum ages for deposition of the lower outwash unit.	QL-1338					29,600±350			-25.0	AA-13845	13,162±102*	-27.9					
				UGA-6930					28,550±480			-25.0	AA-13840	13,024±88*	-27.3					
		19	Puerto Montt. Top of peat layer that separates two glaciofluvial units stacked against the gulfside ice-contact slope. The peat bed signifies ice recession. Upper surface of the peat bed preserved intact beneath glaciofluvial unit; its age therefore signifies ice advance. The first two dates from top of peat; the third date from bottom.	UGA-6932					29,420±650			-25.0	AA-13840	13,024±88*	-27.3	25	Ditto.	A-8258	13,370±100	-28.4
				QL-4538					29,030±540			-24.3	AA-13842	13,582±94*	-28.4					
		19	Puerto Montt. Same site as above, except a lower peat bed covered by glaciofluvial unit. Dates are from top peat surface and signify glacial advance.	A-7667					29,560±275/-265			-25.6	27	Ditto.	T-9662A	13,935±270	-20.4			
				QL-1339					37,400±500			-26.7	28	Ditto.	31	Estero Huitanque. Gytja from base of core in mire on Llanquihue drift. Minimum age for ice recession following the youngest Llanquihue maximum.	TUa-258A	13,345±105*	-25.8	
		QL-4537	33,900±1020	-26.7					32			Basal gyttja from mire on Llanquihue drift. Minimum age for ice recession following youngest Llanquihue maximum.					T-10307A	13,560±95	-28.2	
19	Puerto Montt. Same site as above, except a lower peat bed covered by glaciofluvial unit. Dates are from top peat surface and signify glacial advance.	A-7664	35,470±680/-625	-25.9	33	Chadmo. Gytja from base of a mire. Minimum age for ice recession.							GX-3809	13,065±320						
		UGA-6926	39,340±2130/-1680	-29.1					34	Puerto Carmen. Gytja from base of a core on side of lake. Minimum age for ice recession.	Beta-10481	13,040±210								
19	Puerto Montt. Same site as above, except a lower peat bed covered by glaciofluvial unit. Dates are from top peat surface and signify glacial advance.	A-7626	23,120±130/-125	-27.9	35	Laguna Chaiguata. Gytja from near base of core taken on side of lake. Minimum age for ice recession.	Beta-10485	13,100±260												
		T-11330A	23,005±120	-27.3			36	Cuesta Moraga. Peat over drift. Minimum age for deglaciation.	RL-1892	12,310±360										
19	Puerto Montt. Same site as above, except a lower peat bed covered by glaciofluvial unit. Dates are from top peat surface and signify glacial advance.	A-7912	24,055±150	-27.2	37	Reworked peat clast in folded outwash in front of outermost Llanquihue moraine. Maximum limiting age for folding and hence for outer Llanquihue moraine.			A-7663	29,265±210/-205	-24.9									
		A-8170	29,680±270/-260	-27.5			38	Peat clast reworked into outwash beneath till of outermost Llanquihue moraine. Maximum age for moraine.	A-6777	29,080±360	-29.3									
20	Taiquemó. Peat from the base of a core in a mire that rests against the outermost Llanquihue moraine. Minimum date for moraine.	A-8171	28,465±225/-245	-27.4	39	Peat clasts reworked into core of outermost Llanquihue moraine. Maximum ages for moraine.			A-6487	26,230±340	-27.0									
		A-8172	30,610±290/-280	-27.0			A-6488	28,970±410	-26.6											
20	Taiquemó. Peat from the base of a core in a mire that rests against the outermost Llanquihue moraine. Minimum date for moraine.	A-7701	29,255±210/-200	-26.7																
		A-7705	29,655±230/-225	-27.4																
20	Taiquemó. Peat from the base of a core in a mire that rests against the outermost Llanquihue moraine. Minimum date for moraine.	A-7913	29,210±210/-205	-26.8																
		AA-14770	>49,892*	-30.0																

\*Accelerator-mass-spectrometry radiocarbon date. +estimated.

B.P.), Fundo Llanquihue (between 20,890 and 14,000  $^{14}\text{C}$  yr B.P.), Dalcahue (30,070 to 14,810  $^{14}\text{C}$  yr B.P.), Puerto Varas (14,500  $^{14}\text{C}$  yr B.P.), and the Punta Penas (16,000  $^{14}\text{C}$  yr B.P.). Pollen abundance suggests that the Subantarctic Parkland environment was characterized by patches of southern beech trees (*Nothofagus cf beturoides*) in an open landscape of grasses and composites. At times, for example between 19,000 and 15,000  $^{14}\text{C}$  yr B.P., communities of beech evidently expanded, forming woodland or forest of limited areal extent, but at no level did beech displace open vegetation. In addition, elements of Magellanic Moorland flora were observed in cores from areas where drainage was impeded. Sources were cushion bogs of *Donatia*, *Astelia*, and *Lepidothamnus*, along with associated scrub of *Drimys*, *Pilgerodendron*, *Empetrum*, *Pernettya*, and *Huperzia*.

Today, many of the former Subantarctic Parkland species of the Lake District and Isla Grande de Chiloé are best represented on poorly drained soils along the outer, cold and wet, rocky coast of southernmost Chile. But that setting does not serve as an adequate modern analogue because the geologic conditions are not comparable. In particular, the thick and extensive alluvial fill of the longitudinal valley of the Lake District is not replicated in the Magellanic Moorland environment of southern Chile. We suggest that the grasses and composites of the glacial-age Subantarctic Parkland became widespread where conditions were suitable for their growth and reproduction on the well-drained outwash plains of the longitudinal valley and eastern Isla Grande de Chiloé. Elements of Magellanic Moorland flora made up the lowland vegetation in boggy areas on moraine belts or where former meltwater spillway channels cut deeply into outwash plains, leaving poorly drained depressions. Overall, the Subantarctic Parkland vegetation required higher-than-present precipitation and mean summer temperatures about 6°C lower than at present. This climate is in accord with the implications of species-poor fossil-beetle assemblages of the last glacial maximum, namely that mean summer temperatures in the Lake District were 4° to 5°C below present values and that Magellanic Moorland elements occurred in poorly drained areas (16).

**Llanquihue glacier collapse.** The deep basins now occupied by lakes and marine gulfs in the longitudinal valley formed when glacier lobes collapsed following the youngest Llanquihue-age glacial maximum. Near Seno Reloncavi, basal organic-rich lacustrine sediments from depressions on Llanquihue drift gave minimum ages of 13,024 to 13,932  $^{14}\text{C}$  yr B.P. (sites 24 to 29) for this glacier collapse. Similar dates on

Isla Grande de Chiloé range from 13,040 to 13,935  $^{14}\text{C}$  yr B.P. (sites 30 to 35). All of these dates come from sites within the limits of the youngest Llanquihue advance. From this suite of dates we can state that glacier recession was certainly underway before 13,500  $^{14}\text{C}$  yr B.P. and most probably by 13,900  $^{14}\text{C}$  yr B.P. (17). If they are correct, these ages bracket the youngest Llanquihue glacial maximum between 14,890 and 13,900  $^{14}\text{C}$  yr B.P. Finally, a radiocarbon date from site 36 shows that Andean glaciers had receded from Isla Grande de Chiloé to within 10 km of their current termini on the continent by 12,310  $^{14}\text{C}$  yr B.P.

Shortly after 14,000  $^{14}\text{C}$  yr B.P. vegetation in the Lake District underwent a transition from the long-lived Subantarctic Parkland to North Patagonian Rain Forest. Arboreal diversification began with the spread of Myrtaceae, *Nothofagus cf dombeyi*, *Lomatia*, *Maytenus*, and other relatively thermophilic, arboreal taxa, which became prominent by 13,900  $^{14}\text{C}$  yr B.P. at the Puerto Octay spillway site, by 13,500  $^{14}\text{C}$  yr B.P. at the Fundo Llanquihue site, and by 13,700  $^{14}\text{C}$  yr B.P. at Alerce. Closed stands of North Patagonian Rain Forest evidently

developed by 13,000  $^{14}\text{C}$  yr B.P. This is in accord with an analysis of fossil beetles in the Lake District (16), which shows that the replacement of a species-poor Magellanic Moorland fauna with a species-rich arboreal fauna began at about 14,000  $^{14}\text{C}$  yr B.P. and was completed before 12,500  $^{14}\text{C}$  yr B.P., when the arboreal beetle fauna was similar to that of today. Farther south on Isla Grande de Chiloé, a pollen record from Mayol (site 30) shows that a rapid rise of *Nothofagus* was underway about 14,000  $^{14}\text{C}$  yr B.P., followed shortly by the incursion of North Patagonian Rain Forest species. At nearby Estero Huitanque on Isla Grande de Chiloé (site 31), fossil remains of the water fern *Azolla filiculoides* appear by about 13,700  $^{14}\text{C}$  yr B.P., indicating a moderated temperate environment early in deglaciation. Relative to the preceding glacial conditions, the temperature rise indicated by the fossil record was  $\geq 4^\circ\text{C}$ . Later, after 12,000  $^{14}\text{C}$  yr B.P., the spread of more cryophilic species in the North Patagonian Rain Forest (*Podocarpus*, *Pseudopanax*) suggests climatic cooling and a reversal of trend until the end of the late-glacial.

Overall, the collapse of Andean pied-

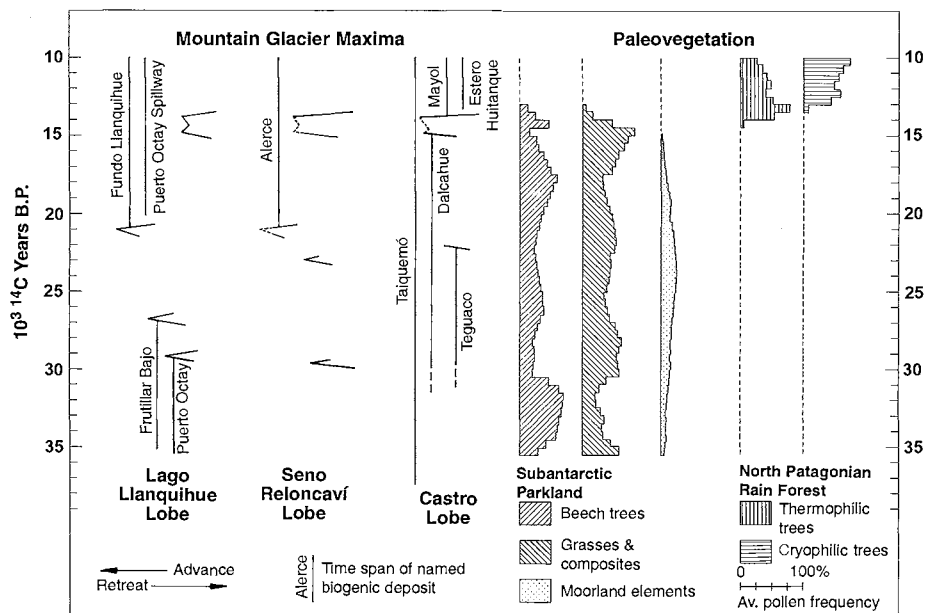


**Fig. 2.** Glacial maxima and overall paleovegetation changes in the Chilean Lake District and Isla Grande de Chiloé. Relative abundance of components in the schematic composite of paleovegetation is derived from 10 individual pollen records of biogenic deposits whose position and age in relationship to the glacial maxima of individual piedmont glacier lobes are shown by the labeled vertical bars. The 10 radiocarbon-dated biogenic deposits show intervals when specific sites in the moraine belt were not glaciated. Fundo Llanquihue is site 12 in Fig. 1 and Table 1; Puerto Octay spillway is site 10; Frutillar Bajo is site 17; Puerto Octay is site 18; Taiquemó is site 20; Dalcahue is site 3; Tequaco is site 15; Mayol is site 30; and Estero Huitanque is site 31. Subantarctic Parkland formed an open landscape, a mosaic of beech (*Nothofagus cf beturoides*) communities, variable in extent, among an expanse of shrubs and herbs, mostly grasses and composites; under conditions of impeded drainage, moorland contained elements of cushion bogs (*Astelia*, *Donatia*, *Lepidothamnus*) and scrub (*Drimys*, *Pilgerodendron*, *Empetrum*, *Pernettya*, *Huperzia*). After 14,000  $^{14}\text{C}$  yr B.P., Subantarctic Parkland was progressively replaced by North Patagonian Rain Forest, at first with a large, comparatively thermophilic component (Myrtaceae, *Nothofagus cf dombeyi*, *Lomatia*, *Maytenus*), and later after 12,000  $^{14}\text{C}$  yr B.P. by a more cryophilic component (*Podocarpus*, *Pseudopanax*).

mont glaciers began about 14,000  $^{14}\text{C}$  yr B.P. and was accompanied by a vegetational transition from Subantarctic Parkland to North Patagonian Rain Forest. This shift represents the most dramatic environmental change that we have yet recognized in our combined glacial and pollen records. Much of the temperature recovery from glacial to interglacial conditions occurred during this brief transition. We take this important event to be the first major step in the termination of the Llanquihue glaciation.

**Southern Alps of New Zealand.** The Southern Alps glacier system showed the same fundamental behavior as the Chilean piedmont glacier lobes during the last (Oti-ran) glaciation. The Kumara 2<sub>2</sub>, 3<sub>1</sub>, and 3<sub>2</sub> ice limits represent advances to positions at or close to the last glacial maximum, the earliest recognized Kumara 2<sub>2</sub> advance began shortly after 23,500  $^{14}\text{C}$  yr B.P. (18–21). The youngest advance (Kumara 3<sub>2</sub>) culminated at 14,000 to 15,000  $^{14}\text{C}$  yr B.P., and was followed by massive ice recession that left mountain-front lakes in basins formerly occupied by piedmont glacier lobes (18–20). Within this framework are two chronologic details not yet recognized in the Chilean Andes. First, the classic moraine sequence of the former Taramaku glacier system on the west flank of the Southern Alps records a Kumara 2<sub>2</sub> maximum at 17,720  $^{14}\text{C}$  yr B.P. (22, 23). Consistent with this age is the observation that the upper portion of outwash graded to the outer Kumara 2<sub>2</sub> moraine system in the adjacent Grey River Valley was deposited after 18,780  $^{14}\text{C}$  yr B.P. (24). Here a lower outwash unit was deposited just prior to 19,740  $^{14}\text{C}$  yr B.P., suggesting

that glaciers were extensive at this time as well (24). The second point is that the Franz Josef Glacier underwent an advance to the prominent Waiho Loop terminal moraine on the western flank of the Southern Alps at 11,050  $^{14}\text{C}$  yr B.P. (25), and that a moraine remnant in the upper Cropp River Valley dates to 10,055  $^{14}\text{C}$  yr B.P. (26).

**Interhemispheric symmetry.** As discussed above, we recognize major fluctuations for individual Andean piedmont glacier lobes (Fig. 2). Because these glacial terrestrial sequences are typically discontinuous, we combined the individual records into a composite diagram (Fig. 3). Our justification is that the different lobes exhibited consistent behavior where the records overlap. We have also added the advances recorded in New Zealand at 17,720, 11,050, and 10,055  $^{14}\text{C}$  yr B.P. to the composite diagram where the Chilean record has not yet been fully investigated (22, 26). Our justification is that the Chilean Andes and Southern Alps are both in the zone of Southern Hemisphere westerlies without an intervening land mass and that their glacial sequences are similar where they overlap.

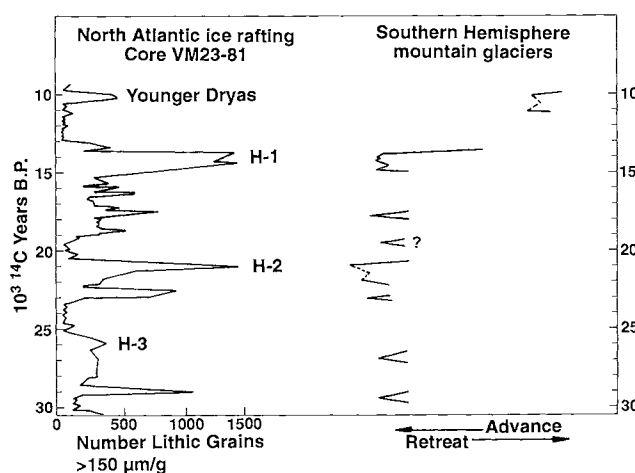
The Southern Hemisphere glacial maxima match ice-rafting peaks derived for the North Atlantic Ocean by Bond and Lotti (27) within the range of error associated with radiocarbon dating (Fig. 3). In both hemispheres, the buildup to the H-2 peak was underway about 22,000  $^{14}\text{C}$  yr B.P.; the peak itself occurred close to 21,000  $^{14}\text{C}$  yr B.P. and the decline at 21,000 to 20,000  $^{14}\text{C}$  yr B.P. Shortly before the H-2 event an earlier glacier peak occurred in both hemispheres at about 23,000  $^{14}\text{C}$  yr B.P. Two peaks also occurred near H-3 in both hemi-

spheres, one at 26,000 to 26,940  $^{14}\text{C}$  yr B.P. and the other at about 29,000 to 29,600  $^{14}\text{C}$  yr B.P. The individual ice-rafting records from Iceland and the Gulf of Saint Lawrence both show a particularly distinct peak in debris at 26,000  $^{14}\text{C}$  yr B.P. (27), close to a maximum of the Lago Llanquihue piedmont lobe. The same situation holds for the ice-rafting peak at 17,500  $^{14}\text{C}$  yr B.P., which for Iceland is particularly prominent and is coeval with the maximum Kumara 2<sub>2</sub> advance of the Taramaku glacier system in New Zealand. Pulses of glacial activity also seem to be coeval in both hemispheres during Younger Dryas time (25, 26).

An apparent exception to the interhemispheric symmetry involves paleoclimatic events in the North Atlantic region leading into the last termination. The ice-rafting record of Bond and Lotti (27) from North Atlantic core VM23-81 shows that the H-1 ice-rafting pulse began about 14,800 to 15,000  $^{14}\text{C}$  yr B.P., culminated at 14,100 to 14,300  $^{14}\text{C}$  yr B.P., and decayed at 13,700  $^{14}\text{C}$  yr B.P. Nearly the same sequence is shown by mountain glaciers in the Chilean Andes, which held a maximum from 14,890 to after 14,240  $^{14}\text{C}$  yr B.P. and which had begun to decay by 13,900  $^{14}\text{C}$  yr B.P. Thus, the last Llanquihue maximum in the Chilean Andes was synchronous with the H-1 ice-rafting pulse in the North Atlantic Ocean. The subsequent recession in both regions is compatible with widespread glacier collapse documented elsewhere in both polar hemispheres at close to 14,000  $^{14}\text{C}$  yr B.P. (18–20, 28–33). It also matches the initial warming shown in the Huascarán tropical ice core from Peru, as calibrated by a radiocarbon chronology transferred from an Atlantic deep-sea core (34). We take this widespread glacial recession and climatic warming to signal the beginning of the last termination. In apparent contradiction to this finding, the first major warming seen in Greenland ice cores occurred abruptly at the beginning of Bölling time about 12,700  $^{14}\text{C}$  yr B.P. (1–3). This early Bölling warming is registered from Greenland across Europe in ice core (1–3), Nordic sea-surface temperature (35), beetle (36), and lacustrine paleoenvironment records (37). The apparent contradiction with the glacial record is resolved, however, if the early Bölling warming is seen as a change in the sites of deep convection in the North Atlantic involving resumption of the modern mode of deepwater production in the Nordic Seas. Such a rearrangement of convection would rapidly increase temperatures in the northern North Atlantic region (38). This interpretation of the overall paleoclimatic record implies that the major North Atlantic thermohaline switch occurred about 1300  $^{14}\text{C}$  years after the abrupt beginning of the last termination on a global scale.

**Fig. 3.** Mountain glacier maxima in the Chilean Andes and in the Southern Alps of New Zealand compared with ice-rafting peaks in the North Atlantic Ocean from Bond and Lotti (27). The Southern Hemisphere mountain glacier peaks during the Younger Dryas and at 17,700  $^{14}\text{C}$  yr B.P. are from the Southern Alps of New Zealand (25, 26). The questionable peak at 19,500  $^{14}\text{C}$  yr B.P. in New Zealand and Chile comes from (15) and (24). All other peaks are from the Chilean Andes as reported here. Overall, there is a striking match between the records.

The main differences come at H-3 (about 26,000  $^{14}\text{C}$  yr B.P. for core VM23-81 and 26,940  $^{14}\text{C}$  yr B.P. for the Lago Llanquihue ice lobe) and at the maximum before H-3 (about 29,000  $^{14}\text{C}$  yr B.P. for core VM23-81 and 29,360 to 29,600  $^{14}\text{C}$  yr B.P. for the Lago Llanquihue and Seno Reloncaví ice lobes) (17, 27). These small differences may be due in part to the method of reducing a series of radiocarbon dates of contemporary material (17). Also, there is some scatter in the age assignments in various North Atlantic cores. For example, the ice-rafting peak before H-3 is placed at about 29,700  $^{14}\text{C}$  yr B.P. in the core from DSDP site 609 (27) rather than at 29,000  $^{14}\text{C}$  yr B.P. as in core VM23-81.



**Implications for global climate change.** The implication of global symmetry that arises from our Southern Hemisphere paleoclimatic data underscores a fundamental lack of understanding of how rapid climatic changes originated and were propagated globally. The millennial-scale glacial pulses registered in both polar hemispheres are too frequent to be explained by Milankovitch orbital forcing. Basally lubricated surges of the Laurentide Ice Sheet (8) are an insufficient explanation because North Atlantic ice-rafting peaks are synchronous among individual ice caps and ice sheets (27) and with the Southern Hemisphere glacier maxima (Fig. 3). Moreover, the global glacial pulses implied by this correlation are not obviously connected with known thermohaline switches in the North Atlantic Ocean. As noted (25), the Younger Dryas-age glacier readvance in New Zealand is difficult to explain by a switch in North Atlantic deep-water production that does not precede the interhemispheric atmospheric signal. The same difficulty now pertains to the Southern Hemisphere advances at 14,890, 17,720, 21,000, 23,060, 26,940, and 29,600  $^{14}\text{C}$  yr B.P.

Bond and Lotti (27) showed that the North Atlantic Heinrich events are actually part of a long series of ice-rafting pulses that recurred at intervals of 2000 to 3000 years. These ice-rafting peaks were concurrent with the Dansgaard-Oeschger cold events in the atmosphere over Greenland. Thus the Heinrich events are seen as a response to the same climate forcing that produced the Dansgaard-Oeschger cold peaks (27). By extension, the match of North Atlantic ice-rafting peaks with Southern Hemisphere mountain glacier maxima reported here implies that the Dansgaard-Oeschger cold pulses had a global signature. Moreover, the Southern Hemisphere moraine record also shows that the mountain glacier peaks correlative with the Heinrich events are embedded in a long series of similar glacier maxima. For example, the mountain glacier maxima at 17,720, 23,060, and 29,600  $^{14}\text{C}$  yr B.P. are about equivalent in magnitude with those that correlate with Heinrich events. Also, millennial-scale glacier pulses in both hemispheres occurred between 20,000 and 13,000  $^{14}\text{C}$  yr B.P. Thus the mechanism that caused the global glacial pulses continued to operate through this puzzling interval where the structure of the Dansgaard-Oeschger events is lost in the Greenland ice cores.

The interhemispheric symmetry of the abrupt atmospheric event that initiated the last termination at about 14,000  $^{14}\text{C}$  yr B.P. is not easily explained by orbital seasonal forcing, which is in an opposite sense at mid-latitudes in the two polar hemispheres. If orbital forcing was indeed responsible,

then some aspect of a seasonal insolation signal (in classic Milankovitch theory taken to be summer insolation at high northern latitudes) must have been amplified by regional mechanisms into global dominance. But such amplification is hard to achieve through orbital forcing of Northern Hemisphere ice sheets, because their direct thermal impact is restricted in area (39) and because their recession at the beginning of the last termination was synchronous with that of Southern Hemisphere mountain glaciers. It is also difficult to ascribe the initial abrupt climatic shift of the last termination to a major change in ocean circulation (40). As discussed above, the switch to the modern type of deep-water formation in the northern North Atlantic basin apparently did not occur until after bi-hemispheric glacier collapse, when Andean and New Zealand mountain glaciers had already shrunk to a small fraction of their areal extent at the last glacial maximum, and when North Patagonian Rain Forest had replaced Subantarctic Parkland in the Chilean Lake District and on Isla Grande de Chiloé.

The timing and interhemispheric synchrony of the last termination is also hard to reconcile with the conceptual model of Imbrie *et al.* (41), in which large Northern Hemisphere ice sheets are the essential condition for feedbacks that drive the 100,000-year climate cycle of late Quaternary time. For the last glacial-interglacial transition, these feedbacks feature the mechanical instability of grounded ice on continental shelves and the capability of large ice sheets to alter the mode of ocean overturning. The train of events leading to the termination is postulated to have begun when strengthening summer insolation forced recession of southern Laurentide ice. The consequent rise of sea level is thought to have destabilized the grounded ice sheet in the Barents Sea, which initiated rapid deglaciation in the North Atlantic sector. Also, the shrinking Laurentide Ice Sheet so altered wind patterns over the North Atlantic Ocean that it triggered a shift in convection sites to the Nordic Seas, thus initiating the modern mode of thermohaline circulation. Because it changed heat distribution and may have increased the concentration of atmospheric  $\text{CO}_2$ , this mode shift is taken to have been the nonlinear amplifier of orbital forcing that is the immediate cause of the last termination. But from our Southern Hemisphere chronology, we suggest that a change in seasonality with strengthening summer insolation is unlikely to have been the immediate cause for recession of southern Laurentide ice, because mid-latitude Southern Hemisphere alpine glaciers showed identical behavior when summer insolation was weakening. Also, the meltwater spike at 14,500 to 13,700  $^{14}\text{C}$  yr B.P. off the Barents Sea

and western Norway (42) correlates with the H-1 ice-rafting peak elsewhere in the North Atlantic (27) and is itself accompanied by a tongue of ice-rafted dropstones (43). Therefore, we think that this meltwater spike represents a maximum rather than a collapse of the Barents Ice Sheet. Finally, our Southern Hemisphere chronology implies that the beginning of the last termination on a global scale antedated (and therefore could not have resulted from) the switch to the modern mode of North Atlantic deep-water production.

The interhemispheric synchrony indicated by our Southern Hemisphere paleoclimatic record suggests rapid propagation through the atmosphere of late Pleistocene climatic signals. The implication is that the forcing mechanism changed the greenhouse gas content or albedo of the atmosphere. On the grounds that the timing is not consistent with our Southern Hemisphere record, we do not favor forcing mechanisms based on ice sheet dynamics or North Atlantic thermohaline switches. Nor have any convincing explanations emerged as to why such mechanisms would have produced any but regional paleoclimatic events. Rather, the interhemispheric synchrony may implicate varying concentrations of atmospheric water vapor as the immediate source of late Pleistocene climatic changes (44, 45). The dominant water vapor feedback in models of climatic warming from greenhouse gases seems to be controlled largely by temperature (46). Because saturation vapor pressure varies nonlinearly with temperature, it has been suggested that perturbations in tropical sea-surface temperatures, now thought to have changed substantially since the last glaciation (47), could have had global consequences (48). Hence, an explanation for the Southern Hemisphere paleoclimatic changes may well emerge with a more complete understanding of the production and redistribution of atmospheric water vapor and the accompanying effects on global climate.

## REFERENCES AND NOTES

1. S. J. Johnsen *et al.*, *Nature* **359**, 311 (1992).
2. P. M. Grootes, M. Stuiver, J. W. C. White, S. J. Johnsen, J. Jouzel, *ibid.* **366**, 552 (1993).
3. W. Dansgaard, J. W. C. White, S. J. Johnsen, *ibid.* **339**, 532 (1989).
4. G. Bond *et al.*, *ibid.* **365**, 143 (1993).
5. G. Bond *et al.*, *ibid.* **360**, 245 (1992).
6. W. Broecker, G. Bond, M. Klas, E. Clark, J. McManus, *Clim. Dynam.* **6**, 265 (1992).
7. W. S. Broecker, G. Bond, M. Klas, G. Bonani, W. Wolfli, *Paleoceanography* **5**, 469 (1990).
8. D. R. MacAyeal, *Paleoceanography* **8**, 767 (1993).
9. P. U. Clark, *Quat. Res.* **41**, 19 (1994).
10. S. C. Porter, *ibid.* **16**, 263 (1981).
11. We consider the radiocarbon ages of in situ samples collected from an undisturbed old land surface buried intact by glaciogenic sediment flows or outwash to pinpoint a glacial advance. If it occurs within the outer Llanquihue moraine belt, such a surface yields an age for a glacial maximum, as plotted in Figs. 2 and 3. We used a simple error-weighted mean age of

- all the samples from each such surface as the date used in the text and in Figs. 2 and 3. We list these values below. Where applicable, we also list in parentheses the error-weighted means calculated for each series of dates after rejecting ages with the largest individual chi-square values. Our procedures follow those set out in G. K. Ward and S. R. Wilson, *Archaeometry* **20**, 19 (1978) and in S. R. Wilson and G. K. Ward, *ibid.* **23**, 19 (1981). The results are: Llanquihue (site 1 in Table 1)  $14,886 \pm 37$   $^{14}\text{C}$  yr B.P. ( $14,824 \pm 41$   $^{14}\text{C}$  yr B.P.), Puerto Varas railroad bridge (site 2)  $14,243 \pm 44$   $^{14}\text{C}$  yr B.P. ( $14,283 \pm 57$   $^{14}\text{C}$  yr B.P.), Dalcahue (site 3)  $14,811 \pm 18$   $^{14}\text{C}$  yr B.P. ( $14,791 \pm 20$   $^{14}\text{C}$  yr B.P.), Teguaco (site 15)  $22,297 \pm 40$   $^{14}\text{C}$  yr B.P. ( $22,398 \pm 47$   $^{14}\text{C}$  yr B.P.), Frutillar Bajo (site 17)  $26,936 \pm 71$   $^{14}\text{C}$  yr B.P. ( $26,614 \pm 92$   $^{14}\text{C}$  yr B.P.), Puerto Octay (site 18)  $29,363 \pm 178$   $^{14}\text{C}$  yr B.P., Puerto Montt highest organic bed (site 19)  $23,058 \pm 88$   $^{14}\text{C}$  yr B.P., Puerto Montt second-highest organic bed (site 19)  $29,598 \pm 87$   $^{14}\text{C}$  yr B.P. ( $29,426 \pm 109$   $^{14}\text{C}$  yr B.P.).
12. Previous radiocarbon dates of organic silt from the upper part of the terrace in the Puerto Varas embayment yielded ages between 13,000 and 14,000  $^{14}\text{C}$  yr B.P. at the Bella Vista Bluff site, the railroad bridge site, and the Northwest Bluff site (10, 15). This led to the conclusion that the final Llanquihue-age readvance culminated about 13,000  $^{14}\text{C}$  yr B.P. (10, 15). Our ages on wood and organic silt for the same localities at Bella Vista Bluff (A-6322; T-9656A) and the railroad bridge (AA-7465; AA-7465C; AA-7459B; AA-7460; ETH-13528) gave consistent ages of 14,500 to 13,900  $^{14}\text{C}$  yr B.P., which we accept as being accurate (see Table 1). We were unable to relocate the Northwest Bluff site because of heavy vegetation growth.
  13. Previous radiocarbon dates from the Dalcahue wood bed are  $14,355 \pm 700$  (GX-8686);  $14,970 \pm 210$  (I-12996); and  $15,600 \pm 560$  (GX-9978)  $^{14}\text{C}$  yr B.P. (14).
  14. J. H. Mercer, *Geophys. Mono.* **29** (American Geophysical Union, Maurice Ewing Ser. Vol. 5, Washington, DC, 1984).
  15. J. H. Mercer, *Quat. Res.* **6**, 125 (1975).
  16. A. C. Ashworth and J. W. Hoganson, *Palaeogeography Palaeoclimatol. Palaeoecol.* **101**, 263 (1993).
  17. The dates from sites 24 to 35 in Table 1 all come from the base of organic lacustrine sediments in depressions on drift within the ice limit reached during the youngest Llanquihue maximum. Hence they all should afford limiting values for the ice collapse that initiated the last termination. We consider these basal dates to be preliminary because each represents only one core in an individual depression. We have not yet checked the reproducibility of our results by obtaining multiple ages from several cores that penetrate basal organic debris within an individual depression. We also point out that dates of  $14,270 \pm 170$   $^{14}\text{C}$  yr B.P. (Beta-67039) and  $14,350 \pm 240$   $^{14}\text{C}$  yr B.P. (Beta-67029) were obtained from near the base of sediment cores at Mayol (site 30) and Estero Huitanque (site 31), respectively. Until they are replicated, however, these dates are not used because they occur slightly higher in the cores than dates of  $13,935 \pm 270$  (T-9662A) and  $13,345 \pm 105$  (TUa-258A)  $^{14}\text{C}$  yr B.P. from Mayol and Estero Huitanque, respectively.
  18. R. P. Suggate, *N.Z. Geol. Surv. Bull.* **77**, 1 (1965).
  19. R. P. Suggate, Ed., *The Geology of New Zealand* (Government Printer, Wellington, New Zealand, 1978), two volumes.
  20. R. P. Suggate and N. T. Moar, *N. Z. J. Geol. Geophys.* **13**, 742 (1970).
  21. We found an interstadial bed overlain by till of the Okarito Formation on the southern flank of Mount Hercules on the west coast of New Zealand in the Kumara  $2_2$  moraine belt. Three wood samples from the top of this bed yielded ages of:  $23,870 \pm 330$  (A-6188),  $23,560 \pm 370$  (A-6591), and  $23,510 \pm 350$  (A-6592)  $^{14}\text{C}$  yr B.P. We think it likely that the glacial advance represented by the overlying till occurred shortly after this time. In addition, Suggate (78) recognized an advance of the Taramaku glacier system into the Arnold River Valley at  $22,300 \pm 350$   $^{14}\text{C}$  yr B.P. (NZ-116).
  22. At Dillmanstown close to Kumara on the west coast of New Zealand beside the Southern Alps, the Taramaku glacier system deposited the type sequence of Kumara-age moraines of the Larikins Formation. Buried beneath the outer Kumara  $2_2$  moraine is an organic silt bed about 0.3 m thick. In places the upper surface of the silt bed preserves intact an original grass surface. Our AMS radiocarbon date of a wood fragment from within the silt 3 cm below this surface was  $17,720 \pm 120$   $^{14}\text{C}$  yr B.P. (ETH-11194). We take this to be the age of the Kumara  $2_2$  maximum in this drainage system. Two other radiocarbon samples previously collected at unspecified depths within the organic silt bed yielded ages of  $18,450 \pm 300$  (NZ-4408) and  $17,250 \pm 250$  (NZ-4407)  $^{14}\text{C}$  yr B.P. (23).
  23. N. T. Moar, *N. Z. J. Ecol.* **3**, 4 (1980).
  24. An organic silt layer of 60 cm thickness interbedded within Kumara  $2_2$  outwash at Raupo within the Grey Valley previously yielded radiocarbon ages from unspecified depths of  $18,600 \pm 290$  (N2-891) and  $18,750 \pm 180$  (NZ-737)  $^{14}\text{C}$  yr B.P. (20). Additional samples that we collected from a new face in the same borrow pit yielded ages of  $19,740 \pm 150$  (A-6550) for the base of the organic silt,  $18,940 \pm 170$  (A-6551) for the middle of the organic silt, and  $18,780 \pm 170$  (A-6552)  $^{14}\text{C}$  yr B.P. for the top of the organic silt. The implication is that deposition of Kumara  $2_2$  outwash at this site ceased at  $19,740$   $^{14}\text{C}$  yr B.P. and was renewed at  $18,780$   $^{14}\text{C}$  yr B.P.
  25. G. H. Denton and C. H. Hendy, *Science* **264**, 1434 (1994).
  26. Whether the Younger Dryas affected the Southern Hemisphere is controversial. For example, see V. Markgraf, *Boreas* **20**, 63 (1991), A. C. Ashworth and V. Markgraf, *Revista Chilena de Historia Natural* **62**, 61 (1989), and L. G. Thompson *et al.*, (34). The structure for the Younger Dryas glacial maximum shown in Fig. 3 comes from New Zealand. A readvance of the Franz Josef Glacier is dated at  $11,050$   $^{14}\text{C}$  yr B.P. (25). A late-glacial moraine in the upper Cropp River Valley was dated to  $10,250$   $^{14}\text{C}$  yr B.P. by L. R. Basher and M. McSeveney *R. Soc. N.Z.* **19**, 263 (1989). We have obtained an error-weighted mean age of  $10,055 \pm 29$   $^{14}\text{C}$  yr B.P. for five additional wood samples from the Cropp River moraine remnant.
  27. G. Bond and R. Lotti, *Science* **267**, 1005 (1995).
  28. D. B. Booth in *North America and Adjacent Oceans During the Last Deglaciation*, H. E. Wright Jr., and W. F. Ruddiman, Eds. (Geological Society of America, Boulder, CO, 1987), pp. 71–90.
  29. C. J. Heusser, *Quat. Res.* **3**, 284 (1973).
  30. A. K. Hansel and W. H. Johnson, *Sveriges Geologiska Undersökning, Ser. Cs* **81**, 133 (1992).
  31. L. C. K. Shane and K. H. Anderson, *Quat. Sci. Rev.* **12**, 307 (1993).
  32. C. Schlüchter, *Bull. Assoc. Franc. l'étude Quat.* **2/3**, 141 (1988).
  33. B. G. Andersen, in *The Last Great Ice Sheets*, G. H. Denton and T. J. Hughes, Eds. (Wiley-Interscience, New York, 1981), pp. 1–65.
  34. L. G. Thompson *et al.*, *Science* **269**, 46 (1995).
  35. S. J. Lehman and L. D. Keigwin, *Nature* **356**, 757 (1992).
  36. T. C. Atkinson, K. R. Briffa, G. R. Coope, *ibid.* **325**, 587 (1987).
  37. U. Siegenthaler, V. Eicher, H. Oeschger, W. Dansgaard, *Ann. Glaciol.* **5**, 149 (1984).
  38. S. Rahmstorf, *Nature* **372**, 82 (1994).
  39. S. Manske and A. J. Broccoli, *J. Geophys. Res.* **90**, 2167 (1985).
  40. W. S. Broecker and G. H. Denton, *Geochim. Cosmochim. Acta* **53**, 2463 (1989).
  41. J. Imbrie *et al.*, *Paleoceanography* **8**, 699 (1993); J. Imbrie *et al.*, *ibid.* **7**, 701 (1992).
  42. M. Sarnthein *et al.*, in *The Last Deglaciation: Absolute and Radiocarbon Chronologies*, E. Bard and W. S. Broecker, Eds. (Springer-Verlag, Berlin, 1992), pp. 183–200.
  43. J. F. Bischof, *Mar. Geol.* **117**, 35 (1994).
  44. G. Bond, unpublished manuscript.
  45. W. S. Broecker, *Nature* **372**, 421 (1994).
  46. A. D. Del Genio, A. A. Lacies, R. A. Ruedy, *ibid.* **351**, 382 (1991).
  47. T. P. Guilderson, R. G. Fairbanks, J. L. Rubenstone, *Science* **263**, 663 (1994).
  48. D. Peteet *et al.*, *Eos* **74**, 587 (1993).
  49. J. T. Hollin and D. H. Schilling, in *The Last Great Ice Sheets*, G. H. Denton and T. J. Hughes, Eds. (Wiley-Interscience, New York, 1981), pp. 179–206.
  50. C. J. Heusser, *Rev. Geol. Chile* **17**, 3 (1990).
  51. C. Villagrán, *Quat. Res.* **29**, 294 (1988).
  52. Supported by the Office of Climate Dynamics of the National Science Foundation (NSF), the National Geographic Society, the National Oceanic and Atmospheric Administration, the Norwegian Research Council, and the Swiss National Science Foundation. The field work was carried out in cooperation with the Servicio Nacional de Geología y Minería, Santiago, Chile. We thank G. Bond and R. Lotti for the ice-rafting data in Fig. 3. R. Kelly drafted the figures. C. Latorre, A. Moreira, and A. Silva helped in the field. C. Porter built field equipment and helped in the field work. Y. Hechenleitner and M. Boegel helped with local arrangements. C. Villagrán, University of Chile, provided laboratory facilities and guidance during the preparation of the pollen record from the spillway channel site near Puerto Octay. R. Suggate showed Denton many key sites in New Zealand, and W. Broecker invited him on the field trip to South America that initiated this work. We thank C. Eastoe, W. Beck, M. Stuiver, T. Jull, A. Hogg, R. Kailin, G. Bonani, and I. Hajdas for providing radiocarbon dates. R. Lotti archived many of the cores at the Lamont-Doherty Earth Observatory of Columbia University, Palisades, NY, under NSF grant OCE 91-01689 and Office of Naval Research grant N00014-90-J-1060. G. Bond, W. Broecker, G. Jacobson, and two reviewers improved the manuscript markedly.

24 November 1994; accepted 11 August 1995